Hindawi
Mathematical Problems in Engineering
Volume 2019, Article ID 3613651, 14 pages
https://doi.org/10.1155/2019/3613651

Research Article

A Novel Seismic Risk Analysis Method for Structures with Both Random and Convex Set Mixed Variables: Case Study of a RC Bridge

Xiao-Xiao Liu [1,2] **and Yuansheng Wang** [2]

[1] *State Key Laboratory for Strength and Vibration of Mechanical Structures, School of Aerospace Engineering, Xi'an Jiaotong University, Xi'an 710049, China*
[2] *Department of Mechanical and Civil Engineering, Northwestern Polytechnical University, Xi'an, 710129, China*

Correspondence should be addressed to Xiao-Xiao Liu; xxliu1989@xjtu.edu.cn
and Yuansheng Wang; wangyuansheng@nwpu.edu.cn

Received 3 July 2018; Revised 27 November 2018; Accepted 2 December 2018; Published 3 January 2019

Academic Editor: Giovanni Minafò

Copyright © 2019 Xiao-Xiao Liu and Yuansheng Wang. This is an open access article distributed under the Creative Commons Attribution License, which permits unrestricted use, distribution, and reproduction in any medium, provided the original work is properly cited.

Assessing the demand hazards of structures is requested in the framework of performance-based earthquake engineering. An efficient method for estimating the seismic risk of structures is proposed in this paper. The relationship between multiple limit capacities and corresponding response parameters is denoted by using a generalized multidimensional limit state equation. The limit states of different components are described as random and convex mixed variables. The seismic responses of different components are considered dependent and follow a multidimensional lognormal distribution. The mathematical formula of multidimensional demand hazards of structures is then derived through combining the seismic fragility function and the seismic hazard curve. The proposed method is used to perform the demand hazard analysis and the parameter sensitivity analysis of a multispan continuous concrete girder bridge, selecting column ductility and bearing displacement as the two-dimensional seismic response parameters obtained by Incremental Dynamic Analysis. The results demonstrate that the coefficient of variation and correlation coefficient N, which are involved in the limit state equation, have an impact on the evaluation of the demand hazards.

1. Introduction

Earthquake disasters frequently occur in the whole world bringing about great damage to the safety of lives and properties of people. Therefore, evaluating the seismic risk of infrastructure and transportation networks has been attracting more and more attention. Risk assessments are often based on probabilistic frameworks [1], due to the existence of uncertainties of ground motion and structural parameters. In this case, a Probabilistic Seismic Demand Analysis (PSDA) is usually adopted to evaluate the demand risk of structures. The principal result of traditional PSDA is the demand hazard curve for a given structure, coupling Probability Seismic Hazard Analysis (PSHA) and nonlinear response analysis [2, 3]. Cornell and Krawinker [4] indicated that the Pacific Earthquake Engineering Research (PEER) Center treated the traditional PSDA as the cornerstone of earthquake resisting behavior evaluation.

The traditional PSDA for RC structures has been investigated for a couple of years, such as Cornell [5], Bazzurro [6], Shome [7], Bazzurro and Cornell [8], Jalayer and Cornell [9], Vamvatsikos and Cornell [10], Mackie and Stojadinović [11], Rathje and Saygili [12], and Eads et al. [13]. A number of scholars have discussed some improved approaches to assess structural demand hazards. In Baker and Cornell [14] the formulation of a drift demand hazard curve was modified by using a vector intensity measure (IM). In Tothong and Cornell [15] an improvement of structural demand hazard curves might be provided via the modified modal pushover analysis and the Mori method. In Tothong and Luco [16] and Tothong [17] probability demand hazard analysis of the drift demand response could be more conservative through

advanced ground motion intensity measures, attenuation relationships, and near-fault effects. In Lv et al. [18] the drift demand hazard curves for two example RC frame structures could not be underestimated, when the uncertainties of structural parameters were considered and an improved cloud method was applied. In addition, there are existing contributions on peak floor accelerations of nonstructural components (e.g., piping systems, infilled walls, and partition walls), such as Miranda and Taghavi [19], Wieser [20], Soroushian et al. [21], and Tian et al. [22].

There are also various studies on the demand risk assessment of bridges. In Mander [23] the risk modeling of maximum drift accounting for uncertainty was applied to seismic financial risk assessment of bridges by adopting a suitable suite of ground motions and performing IDA. In Bradley et al. [24] an improved seismic hazard model was calibrated according to these "exact" hazard data for major centers in New Zealand, and then the new hazard model computed by a semianalytical method would attain more accurate risk assessment results. In Bradley et al. [25] the demand hazard curves of different components (e.g., pile, abutment, and abutment-deck) were obtained through advanced soil and structural constitutive models and then were used to perform probabilistic seismic performance analysis and loss assessment. In Zen et al. [26] the hazard curve of bridge displacement could be improved by using damping devices.

Corresponding contributions on the demand responses of bridge components have been found for several years. In Wilson and Tan [27] a two-part analytical model was developed to assist in seismic response analysis of a highway bridge abutment system, which included the transverse and vertical stiffness characteristics. In Mackie and Stojadinović [28] a probability seismic demand model was used to develop the relationship between spectral displacement and bridge column curvature ductility. In Gardoni et al. [29] the deformation and shear capacities of a single-column bridge bent were subjected to cyclic loads based on a large body of existing experimental observations, and then the univariate and bivariate probabilistic models for the demand responses could be constructed by using a Bayesian framework. In Nielson [30] the force-deformation hysteretic relationships of bridge column and steel bearing were obtained by using nonlinear dynamic analysis, and the respective relationship was applied to assess the seismic risk of MSSS steel girder bridges.

The aforementioned studies focus on the assessment of structural seismic risk and the components' contributions; there is almost the only one Engineering Demand Parameter (EDP) and correspondingly only one limit state. Some literatures [32, 33] emphasized that the limit capacities should be considered as random variables and the seismic performance of structures should be evaluated by using multiple Engineering Demand Parameters (EDPs). Cimellaro and Reinhorn [34] also revealed that the relationship between EDPs and limit capacities should be defined by using a generalized multidimensional limit state (GMLS) equation. However, the definition of limit state based on a combination of probability and convex set mixed models has not been explored in the existing paper. Since the uncertainties in EDPs of different components originated from the same source of uncertainties, multiple response parameters should be treated as dependent quantities. The dependencies between multiple response parameters in the framework of PSDA, as well as the effect of the GMLS, have not been reported so far. The multiple demand hazard function could be constructed by the mathematical "surface," when the multiple EDPs are simultaneously taken into account.

In order to evaluate the multidimensional demand hazards of structures (MDH), the proposed method is applied to a multispan continuous (MSC) concrete girder bridge. The nonlinear dynamic model of the example bridge is established through the OpenSees platform. The column ductility and bearing displacement are selected as two-dimensional EDPs and can be calculated by utilizing Incremental Dynamic Analysis (IDA). The relationship between the two EDPs and their associated limit capacities are defined by a two-dimensional limit state equation (TLS). The two limit capacities are regarded as a probability-convex hybrid model (PCHM). The two dependent EDPs follow a two-dimensional lognormal distribution (TLD). Then the formulation of two-dimensional demand hazard (TDH) can be derived by coupling the TLD and the ground motion hazard curve. The sensitivities of the developed method for evaluating the MDH are discussed when the coefficient of variation (CV) and correlation coefficient N are considered in the GMLS equation.

2. Probabilistic Demand Hazard Assessment (PDHA)

In the framework of traditional PDHA, the mean annual frequency λ of exceeding a given limit level can be obtained by convolving the seismic fragility curve of the structure and the seismic hazard curve of the designated site. The term λ is calculated using the following integral form:

$$\begin{aligned}\lambda_{\psi}(\varphi) &= \int P[\psi > \varphi \mid S_a = im] \left| dH_{S_a}(im) \right| \\ &= \int F_{\psi}(im) \left| dH_{S_a}(im) \right| \\ &= \int F_{\psi}(im) \left| \frac{dH_{S_a}(im)}{d(im)} \right| |d(im)|,\end{aligned} \tag{1}$$

where $\lambda_{\psi}(\varphi)$ is the mean annual frequency of the following example bridge; F_{ψ} is the seismic fragility of the bridge; $H_{S_a}(im)$ is the seismic hazard curve at the site calculated by the Probability Seismic Hazard Analysis (PSHA). In this section, the seismic fragility is defined as a conditional probability that column ductility ψ exceeds a limit capacity φ, given a specific spectral acceleration S_a. The column ductility ψ is obtained by using the following expression:

$$\psi = \frac{\psi_m}{\psi_y}, \tag{2}$$

where ψ is the curvature ductility ratio of bridge column; ψ_m is the maximum curvature under the seismic loading; ψ_y is yield curvature.

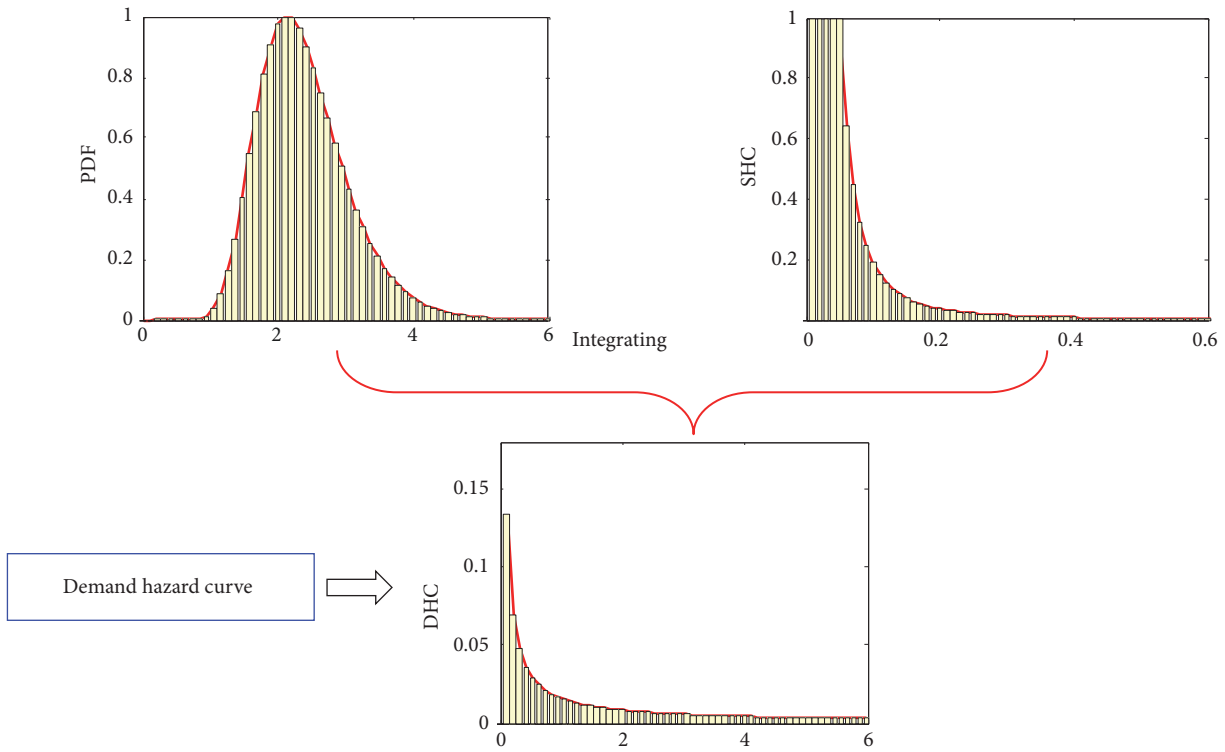

Figure 1: The framework of traditional PDHA.

In the view of Clough and Penzien [35], the peak EDPs (e.g., forces and deformation) follow a lognormal distribution, which is employed to develop positive random variables. Likewise, Cimellaro et al. [36] verified the assumption by comparing different PDF (normal, Gumbel, and lognormal) for different structural configurations and showed that the lognormal distribution is the best fit to the distribution of an EDP. Hence, the maximum column ductility ψ can be assumed to be lognormally distributed:

$$f(\psi \mid im) = \frac{1}{\sqrt{2\pi}\psi\sigma_{\psi|im}} * \exp\left\{-\frac{1}{2\sigma_{\psi|im}^2} * \left(\ln\psi - \mu_{\psi|im}\right)^2\right\}, \quad (3)$$

where $\mu_{\psi|im}$ and $\sigma_{\psi|im}$ are the log-mean and the log-standard deviation values. The mean annual frequency can be computed by using the Monte Carlo Simulation (MCS).

$$\lambda_{\psi}(\varphi) = \int P[\psi > \varphi \mid S_a = im] \left|dH_{S_a}(im)\right| = \sum_{j=1}^{\infty} P[\psi > \varphi \mid im_j] \cdot \left|\frac{dH_{S_a}(im_j)}{d(im_j)}\right| \cdot \Delta im \quad (4)$$

$$= \sum_{j=1}^{\infty} \frac{1}{N_{MCS}} I\left[\psi_{im_j} > \varphi^i\right] \cdot \left|\frac{dH_{S_a}(im_j)}{d(im_j)}\right| \cdot \Delta im, \quad (5)$$

where φ^i is the deterministic limit capacity of column ductility under the ith performance level; ψ_{im_j} is the maximum column ductility subjected to a given S_a for the j^{th} Monte Carlo trial; N_{MCS} is the total number of Monte Carlo trials; $I[\bullet]$ is the indicator function which equals 1 when $[\bullet]$ is true or equals 0 if $[\bullet]$ is false. In this paper, the number of Monte Carlo trials of $N_{MCS} = 10^5$ is considered.

Under the assumption of smaller probabilities of exceedance for the site [37], a logarithmic linear relation between the spectral acceleration at the first period of the bridge and $H_{S_a}(im)$ can be described as follows:

$$H_{S_a}(im) = P[S_a > im] = k_0 \cdot (im)^{-k}, \quad (6)$$

where k_0 is constant and is a dependent of the seismicity of an individual site and k is the logarithmic slope of the seismic hazard curve (SHC) after a local fitting.

The result of traditional PDHA is a demand hazard curve (DHC). If the occurrence of earthquakes in time is assumed to be a Poisson process, the probabilistic model for the column ductility hazard curve can be computed as follows:

$$P_{1D}[in\ t\ years] = 1 - \exp\{-\lambda(\varphi)\, t\} \quad (7)$$

and the process of (1) is illustrated graphically in Figure 1.

3. Probabilistic Multidimensional Demand Hazard Assessment (PMDHA)

This study extends the definition of PDHA to be multidimensional and uses $\lambda_{\text{M-D}}$ for PMDHA. Three components are needed to calculate $\lambda_{\text{M-D}}$: the TLD, which realizes the dependencies between column ductility and bearing displacement,

failure domain of the TLS, which gives the relationship between the EDPs and limit capacities defined by PCHM, and the seismic hazard curve, which describes the mean annual frequency of exceeding ground motion intensities at the given site [13]. The result of the PMDHA is a demand hazard surface, which can be obtained by solving the proposed three components.

3.1. Description of Probability-Convex Hybrid Model (PCHM). For the limit capacities of different bridge components involved in epistemic and aleatory uncertainties [38], the definition of limit capacities $\mathbf{X}$ can be given through a PCHM

$$\mathbf{X} = \mathbf{x}(\boldsymbol{\zeta}), \tag{8}$$

where $\mathbf{X} = [x_1(\zeta_1), x_2(\zeta_2), ..., x_N(\zeta_N)]$ represents the random variable; $\boldsymbol{\zeta} = [\zeta_1, \zeta_2, ..., \zeta_{N_\zeta}]$ represents the mean of the random variable, which is defined by using a nonprobabilistic convex model [39]. Note that $\boldsymbol{\zeta}$ is the bounded uncertainty.

An interval and an ellipsoid are two types of the most widely used convex models, which can describe the convex variables [40]. When the independencies among the variables are considered, the interval model is adopted. When several variables are dependent with each other, the ellipsoid model is used. If some variables are independent with each other and other relevant variables exist, the multiellipsoid convex model will be employed.

Assume that the convex variables $\boldsymbol{\zeta}$ are divided into N_E groups, and then $\boldsymbol{\zeta}$ can be expressed as follows:

$$\boldsymbol{\zeta}^{\mathrm{T}} = \left\{\boldsymbol{\zeta}_1^{\mathbf{T}}, \boldsymbol{\zeta}_2^{\mathbf{T}}, \ldots, \boldsymbol{\zeta}_{N_E}^{\mathbf{T}}\right\}, \tag{9}$$

where $\boldsymbol{\zeta}_i$ represents the variables vector of the ith group and $\sum_{i=1}^{N_E} n_i = N_\zeta$.

In the ith group, the uncertain domain $\boldsymbol{\zeta}_i^{\mathrm{I}}$ of the variables $\boldsymbol{\zeta}_i$ is quantified by using a multidimensional ellipsoid.

$$\boldsymbol{\zeta}_i^{\mathrm{I}} = \left[\boldsymbol{\zeta}_i^{\mathrm{L}}, \boldsymbol{\zeta}_i^{\mathrm{R}}\right] = \left\{\boldsymbol{\zeta}_i \mid \left(\boldsymbol{\zeta} - \boldsymbol{\zeta}^{\mathrm{C}}\right)^{\mathrm{T}} \boldsymbol{\Omega}_i \left(\boldsymbol{\zeta} - \boldsymbol{\zeta}^{\mathrm{C}}\right) \le \theta_i^2,\ i = 1, 2, \ldots, N_E\right\}, \tag{10}$$

where $\boldsymbol{\zeta}_i^{\mathrm{L}}$ and $\boldsymbol{\zeta}_i^{\mathrm{R}}$ are the lower bound vector and upper bound vector of uncertain variable $\boldsymbol{\zeta}_i$, respectively; $\boldsymbol{\Omega}_i$ is a symmetric positive-definite matrix determining the size and orientation of the ith ellipsoid and it is called as the characteristic matrix; $\boldsymbol{\zeta}^{\mathrm{C}}$ denotes the central point of the ith ellipsoid; θ_i is a positive real number determining the magnitude of the variability.

The midpoint $\boldsymbol{\zeta}_i^{\mathrm{C}}$ and variance $D(\boldsymbol{\zeta}_i^{\mathrm{I}})$ of $\boldsymbol{\zeta}_i$ are, respectively, defined as [41]

$$\boldsymbol{\zeta}_i^{\mathrm{C}} = \frac{\boldsymbol{\zeta}_i^{\mathrm{L}} + \boldsymbol{\zeta}_i^{\mathrm{R}}}{2}, \qquad D\left(\boldsymbol{\zeta}_i^{\mathrm{I}}\right) = \left(\boldsymbol{\zeta}_i^{\mathrm{W}}\right)^2 = \left(\frac{\boldsymbol{\zeta}_i^{\mathrm{R}} - \boldsymbol{\zeta}_i^{\mathrm{L}}}{2}\right)^2. \tag{11}$$

The covariance of the uncertain vectors is defined:

$$\mathrm{Cov}\left(\boldsymbol{\zeta}_i, \boldsymbol{\zeta}_i\right) = D\left(\boldsymbol{\zeta}_i^{\mathrm{I}}\right)$$
$$\mathrm{Cov}\left(\boldsymbol{\zeta}_i, \boldsymbol{\zeta}_j\right) = \frac{\tan\beta}{1 - \tan^2\beta}\left(D\left(\boldsymbol{\zeta}_i^{\mathrm{I}}\right) - D\left(\boldsymbol{\zeta}_j^{\mathrm{I}}\right)\right), \quad D\left(\boldsymbol{\zeta}_i^{\mathrm{I}}\right) \ne D\left(\boldsymbol{\zeta}_j^{\mathrm{I}}\right), \tag{12}$$

where β is the rotation angle of the ellipse and $i \ne j$.

For a multidimensional convex model, the covariance matrix $\mathbf{C}$ is defined:

$$\mathbf{C} = \begin{bmatrix} \mathrm{Cov}(\boldsymbol{\zeta}_1, \boldsymbol{\zeta}_1) & \mathrm{Cov}(\boldsymbol{\zeta}_1, \boldsymbol{\zeta}_2) & \ldots & \mathrm{Cov}\left(\boldsymbol{\zeta}_1, \boldsymbol{\zeta}_{N_E}\right) \\ \mathrm{Cov}(\boldsymbol{\zeta}_2, \boldsymbol{\zeta}_1) & \mathrm{Cov}(\boldsymbol{\zeta}_2, \boldsymbol{\zeta}_2) & \ldots & \mathrm{Cov}\left(\boldsymbol{\zeta}_2, \boldsymbol{\zeta}_{N_E}\right) \\ \cdots & \cdots & \cdots & \cdots \\ \mathrm{Cov}\left(\boldsymbol{\zeta}_{N_E}, \boldsymbol{\zeta}_1\right) & \mathrm{Cov}\left(\boldsymbol{\zeta}_{N_E}, \boldsymbol{\zeta}_2\right) & \ldots & \mathrm{Cov}\left(\boldsymbol{\zeta}_{N_E}, \boldsymbol{\zeta}_{N_E}\right) \end{bmatrix} \tag{13}$$

and then a multidimensional ellipsoid can be denoted by the following expression:

$$\left(\boldsymbol{\zeta} - \boldsymbol{\zeta}^{\mathrm{C}}\right)^{\mathrm{T}} \mathbf{C}^{-1} \left(\boldsymbol{\zeta} - \boldsymbol{\zeta}^{\mathrm{C}}\right) \le \theta_i^2 \tag{14}$$

when the uncertain variables are independent with each other, $\mathrm{Cov}(\boldsymbol{\zeta}_i, \boldsymbol{\zeta}_j) = 0,\ i \ne j$.

In order to avoid an ill-conditioned covariance matrix, the uncertain variables $\boldsymbol{\zeta}$ (ζ space) should be transformed into a set of regularized variables $\mathbf{U}$ (u space).

$$\mathbf{U}_i = \left(\boldsymbol{\zeta}_i^{\mathrm{W}}\right)^2 = \frac{\boldsymbol{\zeta}_i - \boldsymbol{\zeta}_i^{\mathrm{C}}}{\boldsymbol{\zeta}_i^{\mathrm{W}}}, \quad i = 1, 2, \ldots, N_E. \tag{15}$$

Then the multidimensional ellipsoid is transformed into a u space

$$\mathbf{U}^{\mathrm{I}} = \left\{\mathbf{U} \mid \mathbf{U}^{\mathrm{T}} \mathbf{C}_{\mathbf{U}}^{-1} \mathbf{U} \le \boldsymbol{\theta}^2\right\}, \tag{16}$$

where covariance matrix

$$\mathbf{C}_{\mathbf{U}}^{-1} = \begin{bmatrix} \mathrm{Cov}(\mathbf{U}_1, \mathbf{U}_1) & \mathrm{Cov}(\mathbf{U}_1, \mathbf{U}_2) & \ldots & \mathrm{Cov}\left(\mathbf{U}_1, \mathbf{U}_{N_E}\right) \\ \mathrm{Cov}(\mathbf{U}_2, \mathbf{U}_1) & \mathrm{Cov}(\mathbf{U}_2, \mathbf{U}_2) & \ldots & \mathrm{Cov}\left(\mathbf{U}_2, \mathbf{U}_{N_E}\right) \\ \cdots & \cdots & \cdots & \cdots \\ \mathrm{Cov}\left(\mathbf{U}_{N_E}, \mathbf{U}_1\right) & \mathrm{Cov}\left(\mathbf{U}_{N_E}, \mathbf{U}_2\right) & \ldots & \mathrm{Cov}\left(\mathbf{U}_{N_E}, \mathbf{U}_{N_E}\right) \end{bmatrix}. \tag{17}$$

The correlation coefficient of the uncertain variables is defined:

$$\boldsymbol{\eta}_{\mathbf{U}_i\mathbf{U}_j} = \frac{\mathrm{Cov}\left(\mathbf{U}_i, \mathbf{U}_j\right)}{\sqrt{D\left(\mathbf{U}_i^{\mathrm{I}}\right)}\sqrt{D\left(\mathbf{U}_j^{\mathrm{I}}\right)}}, \tag{18}$$

where $D(\mathbf{U}_i^{\mathrm{I}}) = 1$; $D(\mathbf{U}_j^{\mathrm{I}}) = 1$. Then $\boldsymbol{\eta}_{\mathbf{U}_i\mathbf{U}_j} = \mathrm{Cov}(\mathbf{U}_i, \mathbf{U}_j)$ and the multidimensional ellipsoid can be expressed as

$$\mathbf{U}^{\mathrm{I}} = \left\{\mathbf{U} \mid \mathbf{U}^{\mathrm{T}} \boldsymbol{\eta}_{\mathbf{U}}^{-1} \mathbf{U} \le \boldsymbol{\theta}^2\right\}, \tag{19}$$

where $\boldsymbol{\eta}_{\mathbf{U}}$ is the correlation coefficient located in the u space; $\boldsymbol{\eta}_{\mathbf{U}_i\mathbf{U}_j} = 1$ and $|\boldsymbol{\eta}_{\mathbf{U}_i\mathbf{U}_j}| \le 1$.

3.2. Definition of the Generalized Multidimensional Limit State (GMLS) Equation. A GMLS equation permits considering the relationship between the limit capacities and their corresponding EDPs [34].

$$\mathbf{G}\left(\mathbf{R}, \mathbf{R_{LS}}\right) = \sum_{r=1}^{n} \left(\frac{R_r}{S_{r\mathrm{LS}}}\right)^{N_r} - 1, \tag{20}$$

where R_r is the EDP vector of the rth component (e.g., deformability and strength), $S_{r\mathrm{LS}}$ is the limit capacity vector of the EDP of the rth component, and N_r is the correlation coefficient determining the shape of the n-dimensional surface. Due to the consideration of two EDPs, the GMLS equation can be denoted as a two-dimensional limit state (TLS) equation.

$$\mathbf{G}\left(\mathbf{R}, \mathbf{R_{LS}}\right) = \left(\frac{\psi}{\varphi^i(d)}\right)^{N_1} + \left(\frac{\xi}{\delta^i(b)}\right)^{N_2} - 1, \tag{21}$$

where ψ and ξ are the peak column ductility and peak bearing displacement, respectively; $\varphi^i(d)$ and $\delta^i(b)$ are the limit capacities of the column ductility and bearing displacement, respectively; N_1 and N_2 are correlation coefficients; i represents the performance limit state levels (i=1, 2, 3, 4; 1 denotes Normal Operation level; 2 denotes Immediate Occupancy level; 3 denotes Life Safety level; 4 denotes Collapse Prevention level).

The dependent limit capacities $\varphi^i(d)$ and $\delta^i(b)$, which rely on uncertain mechanical properties, are described through a PCHM. The limit capacities are taken as random variables and follow a lognormal distribution [31]. The mean values of the random variables are treated as convex variables. Probabilistic information for limit capacities of two components is listed in Table 1. The coefficient of variation (CV) for different limit capacities is regarded as alterable. For example, the limit capacities of the two EDPs are deterministic quantities when both coefficients of variation are equal to 0. The same CV to both limit capacities (e.g., 0, 0.1, 0.5, 0.8, and 1.0) will be assigned in this paper. d_N, d_{I}, d_{L}, d_C, b_N, b_I, b_L, and b_C are assumed to be nonprobabilistic convex variables, which are listed in Table 2.

The desired TLS equation guarantees that the two peak EDPs can stay below their respective critical values over a specified duration. If $N_1 = 1$, a sector/triangle acceptable region will be introduced to realize the equivalent between the notion of the TLS equation and treatment of the joint probability density function (JPDF) of the two dependent EDPs. The assumption also leads to a mathematical "surface" of two-dimensional demand hazard (TDH). If $N_A > N_D$ and $N_A > 1$, the above problem will be quite complicated and will not be used to complete the demand hazard assessment. Consequently, (21) can be simplified by the following expression:

$$\mathbf{G}\left(\mathbf{R}, \mathbf{R_{LS}}\right) = \frac{\psi}{\varphi^i(d)} + \left(\frac{\xi}{\delta^i(b)}\right)^{N} - 1, \tag{22}$$

where $\varphi^i(d)$ and $\delta^i(b)$ introduce an ellipsoid/convex acceptable region.

3.3. Demand Hazard Function Based on Two-Dimensional Lognormal Distribution (TLD). Since the uncertainties in both EDPs rooted in the same source of uncertainties, the column ductility and bearing displacement should be regarded as dependent and follow a two-dimensional lognormal distribution (TLD) (**the proof for this important assumption is given in Appendix**). The bivariate PDF is shown as follows:

$$\begin{aligned} f\left(\psi, \xi \mid S_a = im\right) = {} & \frac{1}{2\pi\psi\xi\sigma_{\psi|im}\sigma_{\xi|im}\left(1-\rho^2\right)^{1/2}} \\ & * \left\{\exp -\frac{1}{2\left(1-\rho^2\right)} * \left[\left(\frac{\ln\psi - \mu_{\psi|im}}{\sigma_{\psi|im}}\right)^2 \right.\right. \\ & + \left(\frac{\ln\xi - \mu_{\xi|im}}{\sigma_{\xi|im}}\right)^2 \\ & \left.\left. - 2\rho\left(\frac{\ln\psi - \mu_{\psi|im}}{\sigma_{\psi|im}}\right)\left(\frac{\ln\xi - \mu_{\xi|im}}{\sigma_{\xi|im}}\right)\right]\right\}, \end{aligned} \tag{23}$$

where $\mu_{\psi|im}$ and $\sigma_{\psi|im}$ are the log-mean and the log-standard deviation of column ductility, respectively; $\mu_{\xi|im}$ and $\sigma_{\xi|im}$ are the log-mean and the log-standard deviation of bearing displacement, respectively; ρ is the correlation coefficient between $\ln\psi$ and $\ln\xi$.

The mean vector μ^{T} and covariance Σ of TLD are denoted as

$$\begin{aligned} \boldsymbol{\mu}^{\mathrm{T}} &= \left[\mu_{\psi|im}, \mu_{\xi|im}\right] \\ \boldsymbol{\Sigma} &= \begin{bmatrix} \sigma^2_{\psi|im} & \rho\sigma_{\psi|im}\sigma_{\xi|im} \\ \rho\sigma_{\psi|im}\sigma_{\xi|im} & \sigma^2_{\xi|im} \end{bmatrix}, \end{aligned} \tag{24}$$

where ρ is calculated by the following expression:

$$\widehat{\rho} = \frac{(1/n)\sum_{i=1}^{n}\left[\left(\ln\psi_i\right) \bullet \left(\ln\xi_i\right)\right] - \widehat{\mu}_{\psi|im} \bullet \widehat{\mu}_{\xi|im}}{\widehat{\sigma}_{\psi|im} \bullet \widehat{\sigma}_{\xi|im}}, \tag{25}$$

where $\widehat{\rho}$ is the estimator of the correlation coefficient ρ; n is the number of ground inputs; $\widehat{\mu}_{\psi|im}$ and $\widehat{\sigma}_{\psi|im}$ are the estimators of log-mean and log-standard deviation of column ductility, respectively; $\widehat{\mu}_{\xi|im}$ and $\widehat{\sigma}_{\xi|im}$ are the estimators of log-mean and log-standard deviation of bearing displacement, respectively.

Here, a two-dimensional demand hazard function can be derived by combining the TLD and the ground motion hazard curve $H_{S_a}(im)$

$$\begin{aligned} \lambda_{\text{M-D}} = {} & \int P\left[\psi > \varphi^i(d), \xi > \delta^i(b) \mid S_a = im\right] \\ & \cdot \left|dH_{S_a}(im)\right| = \int\int_{\mathbf{D}} f\left(\psi, \xi \mid S_a = im\right) d\psi\, d\xi \\ & \cdot \left|dH_{S_a}(im)\right| = \int\int_{\mathbf{D}} f\left(\psi, \xi \mid S_a = im\right) d\psi\, d\xi \\ & \cdot \left|\frac{dH_{S_a}(im)}{d(im)}\right| |d(im)|, \end{aligned} \tag{26}$$

Table 1: Limit capacities for different bridge components [31].

Limit capacities of bridge components	NO level		IO level		LS level		CP level	
	Mean	CV	Mean	CV	Mean	CV	Mean	CV
Column ductility (-)	d_N	0.59	d_I	0.51	d_L	0.64	d_C	0.65
Bearing displacement (mm)	b_N	0.60	b_I	0.55	b_L	0.59	b_C	0.65

Table 2: Nonprobabilistic convex variables.

Nonprobabilistic convex variables	Interval range	Convex model description
d_N (-) b_N (mm)	$[1.27^1\ 1.29^2]$ $[26.7^1\ 28.9^2]$	$\left[d_N - d_N^C, b_N - b_N^C\right] \begin{bmatrix} 0.538 & 2.362E-2 \\ 2.362E-2 & 0.682 \end{bmatrix} \left[d_N - d_N^C, b_N - b_N^C\right]^{\mathbf{T}} \le 1$
d_I (-) b_I (mm)	$[1.9^1\ 2.10^2]$ $[102.2^1\ 104.2^2]$	$[d_I - d_I^C, b_I - b_I^C] \begin{bmatrix} 0.649 & 5.839E-2 \\ 5.839E-2 & 0.770 \end{bmatrix} [d_I - d_I^C, b_I - b_I^C]^{\mathbf{T}} \le 1$
d_L (-) b_L (mm)	$[3.32^1\ 3.52^2]$ $[134.1^1\ 136.1^2]$	$[d_L - d_L^C, b_L - b_L^C] \begin{bmatrix} 0.826 & 7.947E-2 \\ 7.947E-2 & 0.898 \end{bmatrix} [d_L - d_L^C, b_L - b_L^C] \le 1$
d_C (-) b_C (mm)	$[5.04^1\ 5.24^2]$ $[184.6^1\ 186.6^2]$	$[d_C - d_C^C, b_C - b_C^C] \begin{bmatrix} 0.911 & 8.815E-2 \\ 8.815E-2 & 0.965 \end{bmatrix} [d_C - d_C^C, b_C - b_C^C]^{\mathbf{T}} \le 1$

1 = lower bound determined by IDA; 2 = upper bound obtained by Nielson and DesRoches [31].

where $\lambda_{\text{M-D}}$ is the mean annual frequency of exceeding two dependent limit capacities;

$$\mathbf{D} = \frac{\psi}{\varphi^i(d)} + \left(\frac{\xi}{\delta^i(b)}\right)^N - 1 \ge 0. \tag{27}$$

Likewise, the process of (26) is illustrated graphically in Figure 2.

4. Case Study

4.1. Bridge Geometry. To demonstrate the proposed method for assessing TDH and provide insights into the sensitivities of the parameters of the TLS equation to $\lambda_{\text{M-D}}$, a sample MSC concrete girder bridge located in northwestern China is used as a case study in this paper. As shown in Figure 3, both the end spans and the interior span of this three-span bridge are 11.90 m and 22.30 m. Each bent consists of three circular columns with a 641.2 mm^2 cross-sectional area, reinforced with 12 No. 29 longitudinal bars and No. 13 transverse stirrups spaced at 305 mm. The decks are constructed of eight AASHTO concrete girders, which are Type I for the end spans and Type III for the middle span [42]. The typical bridge uses elastomeric pads for bearings. The girders for the example bridge are made continuous by embedding a concrete parapet between the girders [43]. The foundations are assumed to lie on medium hard soil represented by site class II (i.e., shear wave velocity between 250 m/s and 500 m/s) [44].

4.2. Finite-Element Modeling of a MSC Concrete Girder Bridge. A nonlinear three-dimensional model of the example bridge is created using the finite-element platform OpenSees [45]. For the superstructure modeling, the composite actions of the slab and girder section are modeled using linear elastic beam-column elements, because the superstructure is expected to remain linear. The deck section can be modeled through an equivalent homogeneous concrete material. The detailed equivalent parameters are given by Nielson and DesRoches [42]. The columns and bent beams are modeled by using nonlinear beam-column elements with fiber defined cross sections. The concrete material is modeled using the Kent-Scott-Park model with no tension stiffening. The reinforcing steel is modeled as a bilinear material using Steel01 material. The bearings are modeled using nonlinear translational springs and the elastomeric pads are modeled through an elastic-perfectly plastic material. The pile-bent abutment type in this study is modeled based on the work by Nielson and DesRoches [42]. The fundamental mode for the MSC concrete girder bridge is 1.0056 sec. Meanwhile, the Rayleigh damping coefficient can be calculated by selecting the modal calculations of the 10th and 22nd order. Therefore, the calculated damping constants are 0.0317 (10th modal) and 0.0308 (12th modal), respectively.

5. Ground Motion Selection

Ground motion inputs are often chosen from the PEER Center's NGA database [13]. A criterion for selecting ground motions follows that as recommended by Baker and Cornell [46] which fully accounts for magnitude, distance, focal mechanism, and site class. Baker [47] also illustrated that the Conditional Mean Spectrum (CMS) consisting of epsilon

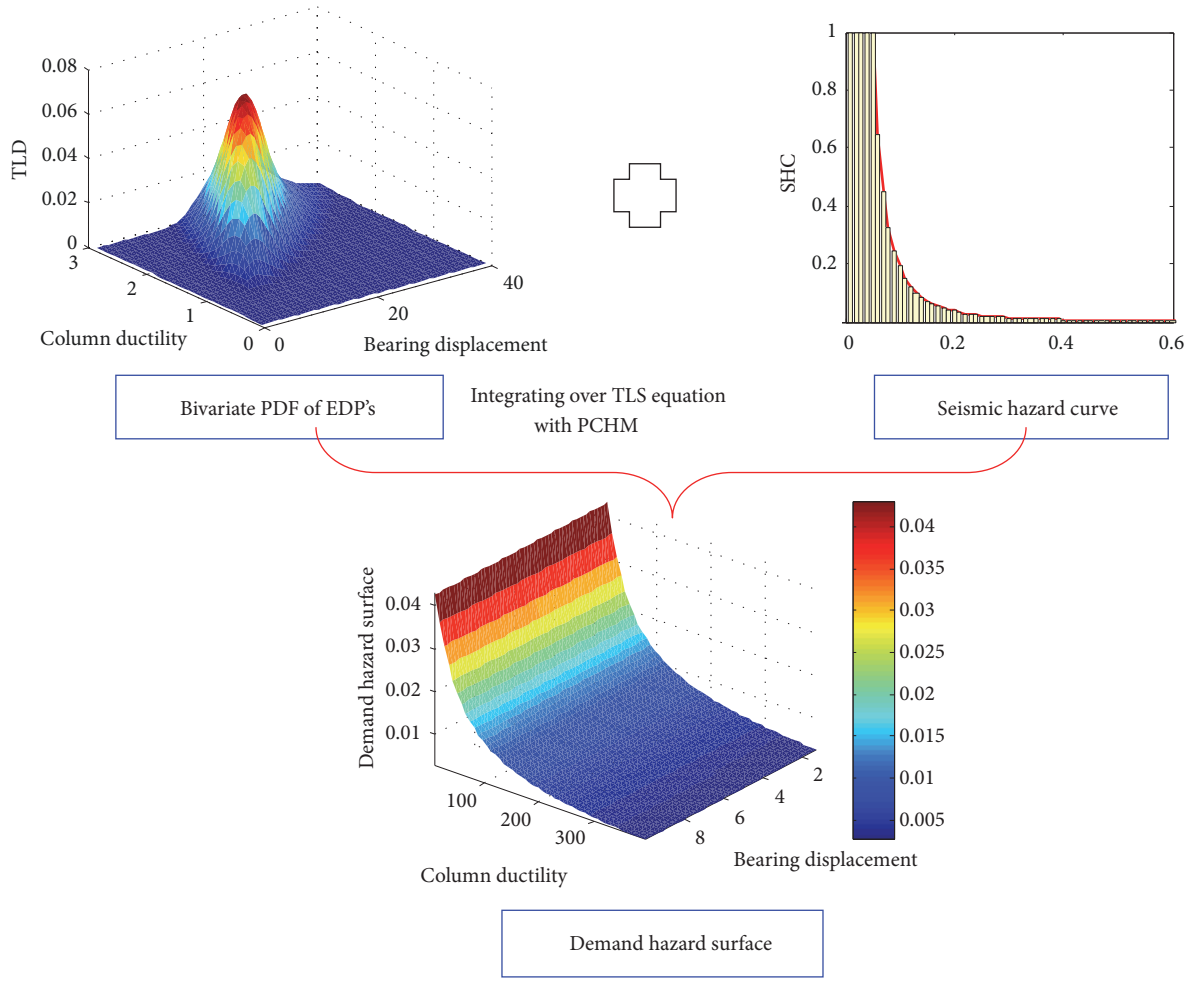

Figure 2: The framework of the proposed PMDHA.

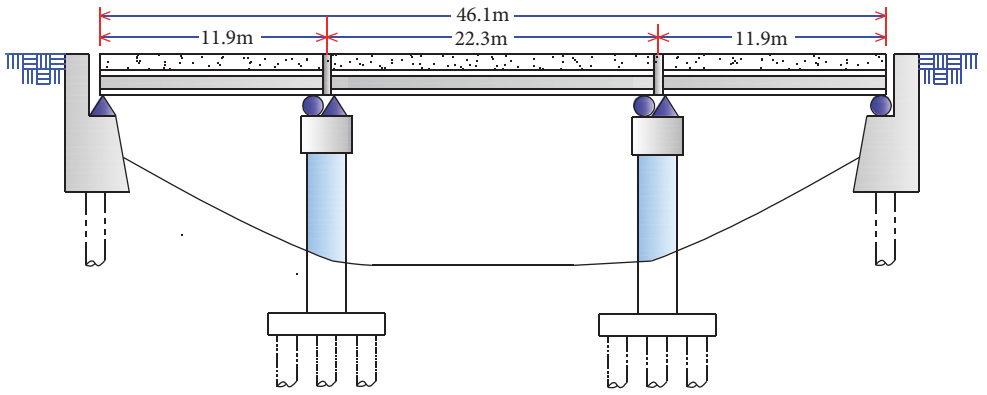

Figure 3: Configuration of the example MSC concrete girder bridge.

and spectral acceleration effectively reduced the dispersion of the structural response. Epsilon is described as an indicator of spectral shape of ground motion records. The detailed computational process of CMS is based on the work by Abrahamson and Silva [48], Baker and Cornell [49], and Baker [47]. The damping constant with respect to ground motion parameters of the seismic zonation maps is calculated as 0.05 based on code GB 18306-2001 [50] or code GB 17741-2005 [51]. Thirty NGA records (M=6-7, R=15-20 km, site class II) have been selected to match the CMS, as shown in Figure 4. These ground motions are able to capture the uncertainty arising from an earthquake when loading to the structures.

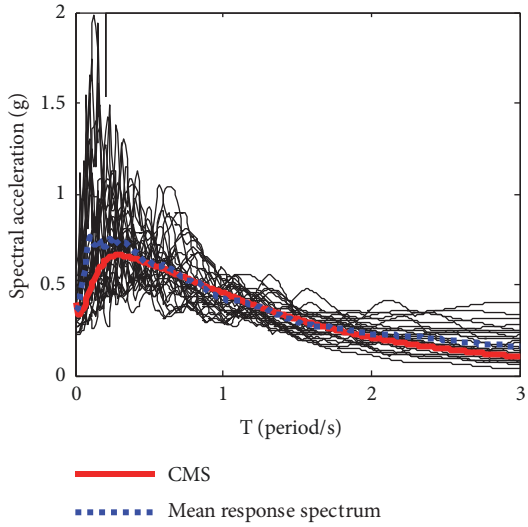

Figure 4: Response spectra of thirty chosen NGA records.

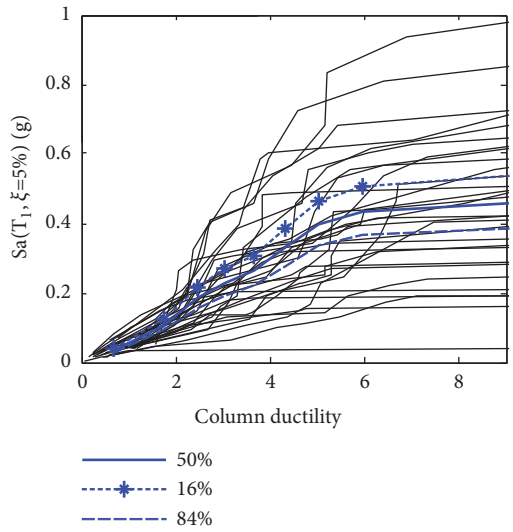

Figure 5: Thirty IDA curves of $S_a(T_1)$ vs. column ductility.

6. Incremental Dynamic Analysis

Incremental Dynamic Analysis (IDA) is a neoteric methodology that offers a distinct relationship between the intensity measure and the demand response. The approach involves performing a sequence of nonlinear dynamic analyses under a multiply scaled suite of recorded ground motions. Each record is scaled to several *IM* levels, which are designed to force the structure all the way from elasticity to finally collapse. Once a series of thirty NGA records selected by the CMS is entered into the finite-element model, IDA can be performed. In order to carry out the analysis, the chosen ground motion records need to be scaled from low *IM* levels to higher *IM* levels until structural collapse occurs. As a result, thirty IDA curves of $S_a(T_1)$ vs. column ductility and $S_a(T_1)$ vs. bearing displacement are presented in Figures 5 and 6, respectively. All of the IDA curves can be assumed to be

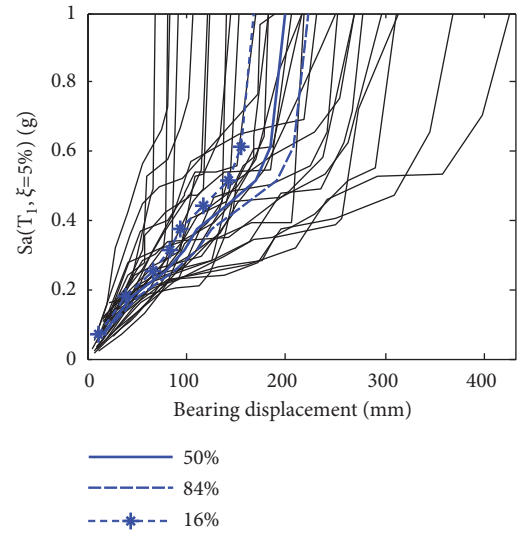

Figure 6: Thirty IDA curves of $S_a(T_1)$ vs. bearing displacement.

a lognormal distribution [23]; hence, the 16%, 50%, and 84% fractile values of $S_a(T_1)$ vs. column ductility and $S_a(T_1)$ vs. bearing displacement are also graphically depicted in Figures 5 and 6, respectively.

7. Designed Site and Seismic Hazard Curve

The geographical location of the example bridge is chosen as northwestern China, because it represents a specific site with smaller probabilities of exceedance. Site class II, eight-times the intensity of the earthquake, and designed ground acceleration for 0.20 are taken into account in this study. Having the knowledge in mind, the hazard–recurrence curve can be obtained by fitting a straight line through two known points in a log–log scale. The parameter k included in (6) is calculated by the following expression:

$$k = \frac{\ln\left(H_{S_1(10\%/50yr)}(S_1)/H_{S_1(2\%/50yr)}(S_1)\right)}{\ln\left(S_{1(2\%/50yr)}/S_{1(10\%/50yr)}\right)}, \quad (28)$$

where $H_{S_1(10\%/50yr)}$ is the probability of exceedance for the 10%/50 hazard level (0.002105), $H_{S_1(2\%/50yr)}$ is the probability of exceedance for the 2%/50 hazard level (0.000404), $S_{1(10\%/50yr)}$ is the spectral amplitude for the 10%/50 hazard level, and $S_{1(2\%/50yr)}$ is the spectral amplitude for the 2%/50 hazard level. Here, $k_0 = 8.0153 \times 10^{-5}$ and $k = 2.3814$.

8. Parameter Sensitivity Analysis

8.1. Sensitivity of CV to Mean Annual Frequency of Exceedance (MAF). Although the coefficients of variation for different limit capacities are given based on Nielson and DesRoches [31], different values of the CV should be used to perform the sensitivity analysis of the MAF. The demand hazard surface can be developed by coupling the TLD and the seismic hazard curve, while the limit capacities are defined using the PCHM. Figure 7 shows the effect of CV on demand hazard surface,

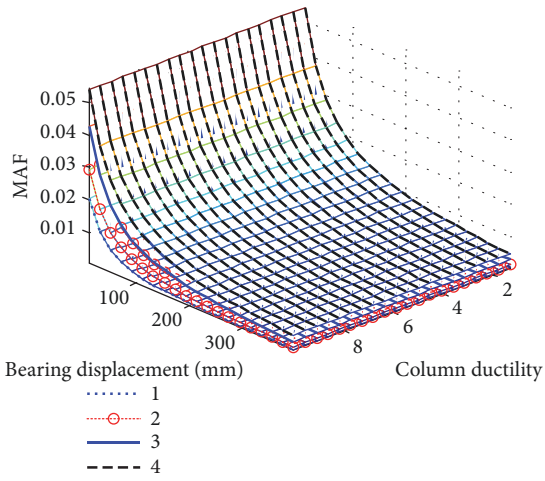

1-CV=0; 2-CV=0.5; 3-CV=Nielson & DesRoches [31]; 4-CV=0.8

Figure 7: Effects of CV on demand hazard surface.

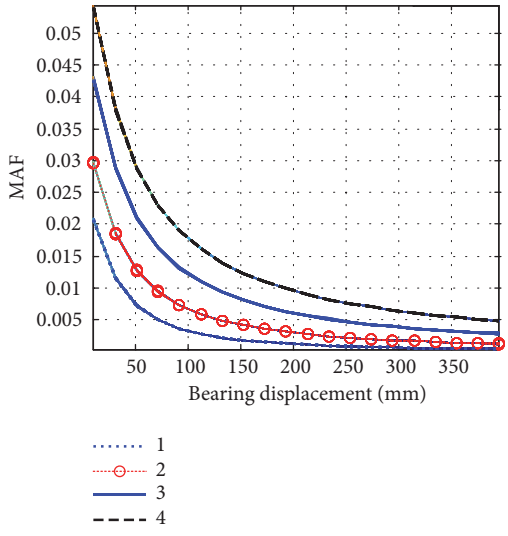

1-CV=0; 2-CV=0.5; 3-CV=Nielson & DesRoches [31]; 4-CV=0.8

Figure 8: Projection of Figure 7 in the Y-Z plane.

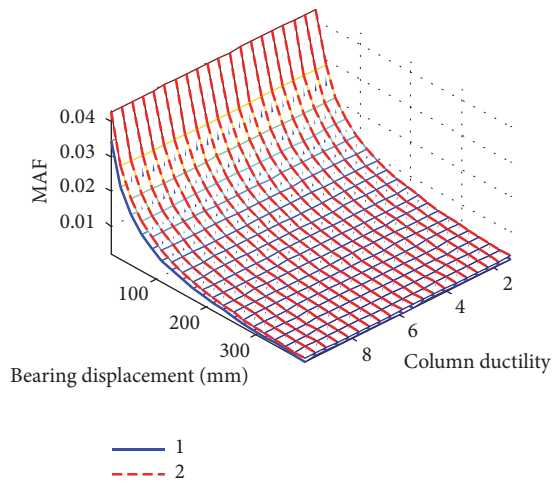

1-limit capacities obtained by Nielson & DesRoches [31];
2-limit capacities defined by PCHM based on Nielson & DesRoches [31]

Figure 9: Discrepancies of demand hazard surfaces between Nielson and DesRoches [31] and PCHM.

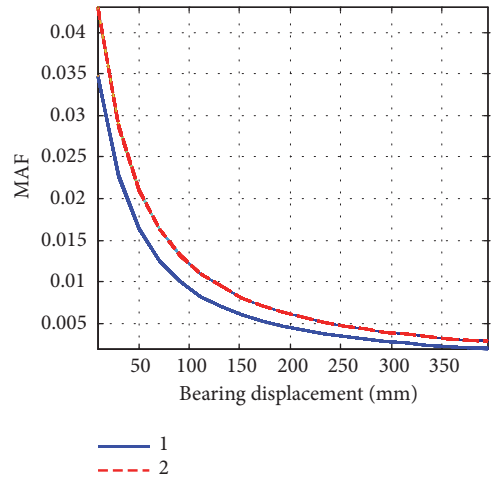

1-limit capacities obtained by Nielson & DesRoches [31];
2-limit capacities defined by PCHM based on Nielson & DesRoches [31]

Figure 10: Projection of Figure 9 in the Y-Z plane.

when the correlation coefficient N involved in (22) is equal to 2. The projection of Figure 7 in the Y-Z plane is presented in Figure 8. From the two figures, it can be observed that the MAF with deterministic limit capacities (CV=0) is lower than if uncertain limit capacities are considered. By comparing with Nielson and DesRoches [31], it can be seen that the MAF will be underestimated if CV $\leq$ 0.5. The results indicate that the CV of limit capacities has a significant impact on the probabilistic demand hazard assessment.

Figure 9 shows the discrepancies of demand hazard surfaces between different definitions of limit capacities when the CV originates in Nielson and DesRoches [31] and N=2. Figure 10 gives the projection of Figure 9 in the Y-Z plane. The two figures reveal that the MAF of the example bridge will be a relatively conservative estimation, if the limit capacities are defined by PCHM.

8.2. Sensitivity of N to Mean Annual Frequency of Exceedance (MAF). The relationship between the limit capacities and EDPs can be described using the TLS equation. The correlation coefficient N determines the shape of (22). For instance, the triangle acceptable region is used when N=1. If N is equal to 2, a regular sector acceptable region will be competent for the description. The irregular acceptable domain occurs when the parameter N is gradually increased. Therefore, an accurate sensitivity analysis of N to MAF is necessary. Figure 11 shows the effects of different values of the parameter N on demand hazard surface when the CV roots in Nielson and DesRoches [31] and the definition of limit capacities originates from PCHM. Meanwhile, the corresponding projection is shown in Figure 12. Results in the two figures show that the MAF of the specific structure will

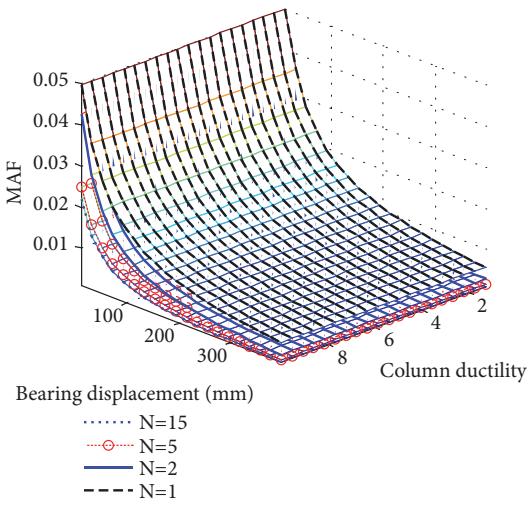

Figure 11: Effects of different values of N on demand hazard surface.

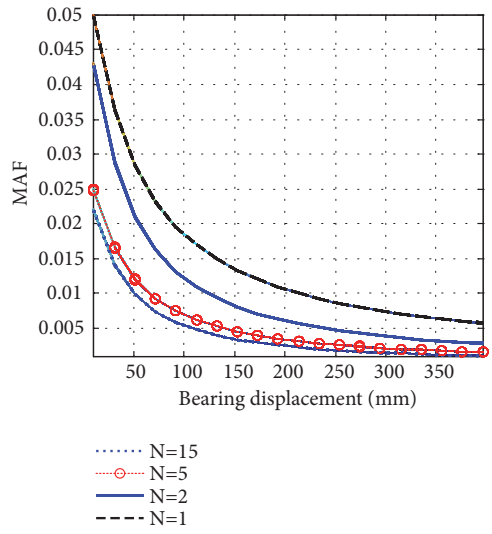

Figure 12: Projection of Figure 11 in the Y-Z plane.

be drastically underestimated, if the parameter N is increased to 15. However, it is noteworthy that the MAF has little difference between N =5 and N =15. This implies that the sensitivity of the parameter will be decreased when N > 5. In summary, the demand hazard surface of the example bridge can be more conservative, if an appropriate correlation coefficient N is assigned.

9. Conclusions

This paper presents an original method to develop the framework of multidimensional demand hazard assessment. The nonlinear dynamic model of a MSC concrete girder bridge is applied to calculate the column ductility and bearing displacement. The dependent two EDPs are assumed to follow the TLD and the limit capacities are defined using PCHM. The curves of $S_a(T_1)$ vs. column ductility and $S_a(T_1)$ vs. bearing displacement are carried out by IDA. One bounded value of convex variables, which are related to mean values of the limit capacities, is determined through 50% fractile values of IDA curves. The other bounded values are obtained resulting from Nielson and DesRoches [31]. Then the relationship between the two EDPs and their associated limit capacities can be constructed using the TLS equation. Subsequently, the demand hazard surface of the example bridge is derived by coupling the TLD and the seismic hazard curve.

From the given numerical example, it can be deduced that MAF of the MSC concrete girder bridge will be undervalued if the uncertainties of the two limit capacities are omitted. Nevertheless, the MAF can be relatively conserved when the CV of uncertain limit capacities is appropriately appointed. Similarly, if an applicable correlation coefficient N is taken into account, more conservative results will be attained. Furthermore, the proposed method has a positive influence on structural risk evaluation, when the limit capacities follow a PCHM, Nielson and DesRoches [31].

Appendix

Proof for Two-Dimensional Lognormal Distribution

Property A.1. Based on the conditional probability formula $P(X, Y) = P(Y \mid X)P(X)$, the necessity and sufficiency of the pair (X, Y) which obeys normal distribution have two parts. Part I: the marginal distribution of the parameter X must be normal distribution.

Part II: the residual error $\boldsymbol{\varepsilon}$ must be normal distribution. $\boldsymbol{\varepsilon}$ can be calculated using linear regression analysis and expressed as follows:

$$\boldsymbol{\varepsilon} = \mathbf{Y} - \mathbf{X}\boldsymbol{\beta}. \tag{A.1}$$

Corollary A.2. *If there exist two lognormal vectors* ln **A** *and* ln **B** *satisfying Property A.1, then the pair* (**A**, **B**) *follows a two-dimensional lognormal distribution.*

Proof. Let $\mathbf{Z} = \begin{bmatrix} e^{\mathbf{X}} \\ e^{\mathbf{Y}} \end{bmatrix} = \begin{bmatrix} \boldsymbol{\psi} \\ \boldsymbol{\delta} \end{bmatrix}$, $\boldsymbol{\mu} = \begin{bmatrix} \mu_1 \\ \mu_2 \end{bmatrix}$, $\sum = \begin{pmatrix} \sum_{11} & \sum_{12} \\ \sum_{21} & \sum_{22} \end{pmatrix}$,

where $\boldsymbol{\psi}$ is the column ductility vector; $\boldsymbol{\delta}$ is the bearing displacement vector; μ_1 is the log-mean of column ductility; μ_2 is the log-mean of bearing displacement; $\sum$ is the covariance matrix.

Cimellaro et al. [36] verified the assumption by comparing different PDF (normal, Gumbel, and lognormal) for different structural configurations and showed that the lognormal distribution is the best fit to the distribution of an EDP. Therefore, ln $\boldsymbol{\psi}$ follows a normal distribution. The pair $(\boldsymbol{\psi}, \boldsymbol{\delta})$ subjected to a given IM level ($S_a(T_1)$ =0.15 g) is obtained through nonlinear dynamic analysis of the FE model, and then these data are used to complete Part I. The result is shown in Figure 13.

MATLAB provides a *lillietest* function to verify the assumption of Part I.

$$[H, P, LSTAT, CQ] = \text{lillietest}\,(X, alpha)\,, \tag{A.2}$$

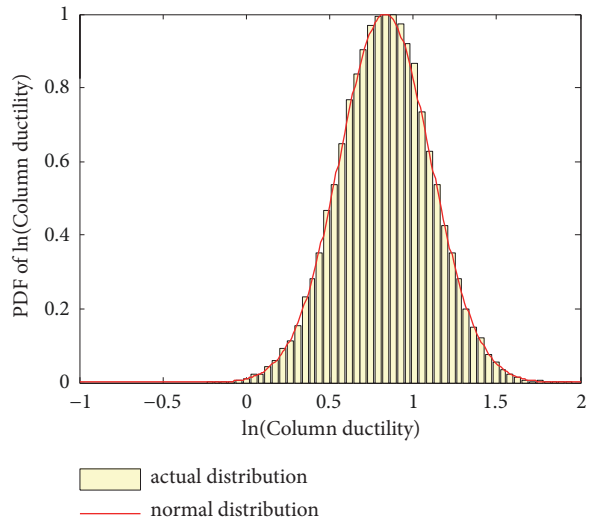

Figure 13: Hypothesis testing of marginal distribution of $\ln \psi$.

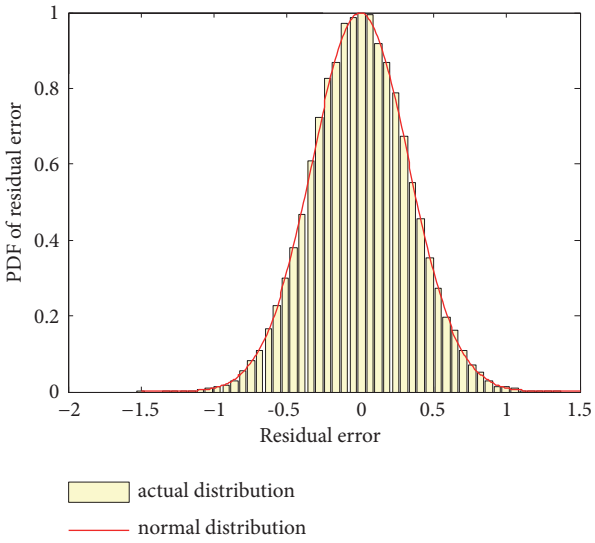

Figure 14: Hypothesis testing of marginal distribution of residual error $\boldsymbol{\varepsilon}$.

where *alpha* is 0.05; *Xis* $\ln \boldsymbol{\psi}$. If H equals 0, the assumption of Part I can be accepted. Performing the *lillietest* function, we have that H is 0; P is 0.2307; *LSTAT* is 0.0033; *CV* is 0.0041.

Likewise, the pair $(\boldsymbol{\psi}, \boldsymbol{\delta})$ is used to complete Part II. The result is shown in Figure 14.

The assumption of Part II can be verified using the *lillietest* function

$$[H, P, LSTAT, CQ] = \text{lillietest}\left(X, alpha\right), \tag{A.3}$$

where *alpha* is 0.05; X is $\boldsymbol{\varepsilon}$. If H equals 0, the assumption of Part II can be accepted. Performing the *lillietest* function, we have that H is 0; P is 0.5000; *LSTAT* is 0.0021; *CV* is 0.0041. Therefore, the results satisfy Corollary A.2. □

Abbreviations and Notations

GMLS: Generalized multidimensional limit state
PCHM: Probability-convex hybrid model
MLD: Multidimensional lognormal distribution
MDH: Multidimensional demand hazards
MSC: Multispan continuous
CV: Coefficient of variation
IDA: Incremental Dynamic Analysis
PSDA: Probabilistic Seismic Demand Analysis
PSHA: Probabilistic seismic hazard analysis
PEER: Pacific Earthquake Engineering Research
EDP: Engineering Demand Parameter
EDPs: Engineering Demand Parameters
TLS: Two-dimensional limit state equation
TLD: Two-dimensional lognormal distribution
TDH: Two-dimensional demand hazard
PDHA: Probabilistic demand hazard assessment
PMDHA: Probabilistic multidimensional demand hazard assessment
MCS: Monte Carlo Simulation
JPDF: Joint probability density function
PDF: Probability density function
SHC: Seismic hazard curve
DHC: Demand hazard curve
NO: Normal Operation level
IO: Immediate Occupancy level
LS: Life Safety level
CP: Collapse Prevention level
CMS: Conditional Mean Spectrum
MAF: Mean annual frequency of exceedance
IM: Intensity measures
λ : Mean annual frequency of exceeding a given limit level
$\lambda_{\psi}(\varphi)$: Mean annual frequency of exceeding a given ductility threshold
F_{ψ}: Seismic fragility function
S_a: Spectral acceleration
$H_{S_a}(im)$: Seismic hazard curve
ψ: Column ductility
φ: Limit capacity of column ductility
ψ_m: Maximum curvature
ψ_y: Yield curvature
ξ: Bearing displacement
δ: Limit capacity of bearing displacement
$f(\psi \mid im)$: Lognormal distribution of the maximum column ductility
$\mu_{\psi|im}$: Log-mean of column ductility
$\sigma_{\psi|im}$: Log-standard deviation of column ductility
φ^i: Deterministic limit capacity of column ductility under the ith performance levels
ψ_{im_j}: Maximum column ductility for the jth Monte Carlo trial

N_{MCS}: Total number of Monte Carlo trials
k_0: Dependent of the seismicity of an individual site
k: Logarithmic slope after a local fitting
$P_{1D}[in\ t\ years]$: Probabilistic model for the column ductility hazard curve
$\mathbf{X}$: Random variable
$\boldsymbol{\zeta}$: Nonprobabilistic uncertain variable, namely, convex variable
$\boldsymbol{\zeta}_i$: The ith nonprobabilistic uncertain variable
$\boldsymbol{\zeta}_i^{\mathrm{L}}$: Lower bound vector of the ith nonprobabilistic uncertain variable
$\boldsymbol{\zeta}_i^{\mathrm{R}}$: Upper bound vector of the ith nonprobabilistic uncertain variable
Ω_i: Symmetric positive-definite matrix of the ith ellipsoid
$\boldsymbol{\zeta}_i^{\mathrm{C}}$: Central point of the ith ellipsoid
$\mathrm{Cov}(\boldsymbol{\zeta}_i, \boldsymbol{\zeta}_i)$: Covariance of the ith uncertain vector
$\mathrm{Cov}(\boldsymbol{\zeta}_i, \boldsymbol{\zeta}_j)$: Covariance between the ith and jth uncertain vector
C: Covariance matrix among uncertain vectors of N_E groups
$\mathbf{U}_i$: ith nonprobabilistic regularized variables (u space)
$\mathbf{C}_{\mathbf{U}}$: Covariance matrix among regularized variables of N_E groups
$\boldsymbol{\eta}_{\mathbf{U}_i\mathbf{U}_j}$: Correlation coefficient between the ith and jth regularized variables
$\mathbf{G}(\mathbf{R}, \mathbf{R}_{\mathbf{LS}})$: Generalized multidimensional limit state equation
$\varphi^i(d)$: Probability-convex variable of limit capacity of column ductility at the ith performance levels
$\delta^i(b)$: Probability-convex variable of limit capacity of bearing displacement at the ith performance levels
d: Convex variable for mean value of limit capacity of column ductility
b: Convex variable for mean value of limit capacity of bearing displacement
N: Correlation coefficient in multidimensional limit state equation
$f(\psi, \xi \mid S_a = im)$: Bivariate lognormal distribution
$\mu_{\xi|im}$: Log-mean of bearing displacement
$\sigma_{\xi|im}$: Log-standard deviation of bearing displacement
ρ: Correlation coefficient between logarithms of column ductility and bearing displacement
μ^{T}: Mean vector of bivariate lognormal distribution
Σ: Covariance of bivariate lognormal distribution
$\widehat{\rho}$: Estimator of the correlation coefficient ρ
n: Number of ground inputs
$\widehat{\mu}_{\psi|im}$: Estimator of log-mean of column ductility
$\widehat{\sigma}_{\psi|im}$: Estimator of log-standard deviation of column ductility
$\widehat{\mu}_{\xi|im}$: Estimator of log-mean of bearing displacement
$\widehat{\sigma}_{\xi|im}$: Estimator of log-standard deviation of bearing displacement
$\lambda_{\text{M-D}}$: Mean annual frequency of exceeding two dependent limit capacities
$\mathbf{D}$: Failure domain of the example bridge.

Data Availability

The data used to support the findings of this study are available from the corresponding author upon request.

Conflicts of Interest

The authors declare that they have no conflicts of interest.

Authors' Contributions

Xiao-Xiao Liu and Yuansheng Wang contributed equally to this work.

Acknowledgments

The authors acknowledge the support of the National Natural Science Foundation of China (grant number 11802224), China Postdoctoral Science Foundation (grant number 2018M633495), China State Key Laboratory for Mechanical Structure Strength and Vibration Open-End Foundation (Grant number SV2019−KF−11), Fundamental Research Funds for the Central Universities (3102016ZY2016), and Aerospace Science and Technology Innovation Fund (2016kc060013).

References

[1] K. A. Porter, "An overview of PEERs performance-based earthquake engineering methodogy," in *Proceedings of 9th International Conference on Applications of Statistics and Probability in Civil Engineering*, San Francisco, Calif, USA, 2003.

[2] N. Luco, *Probabilistic seismic demand analysis, SMRF connection fractures, and near-source effects [Ph.D. thesis]*, Department of Civil Engineering, Stanford University, Calif, USA, 2002.

[3] J. E. Padgett, B. G. Nielson, and R. DesRoches, "Selection of optimal intensity measures in probabilistic seismic demand models of highway bridge portfolios," *Earthquake Engineering & Structural Dynamics*, vol. 37, no. 5, pp. 711–725, 2008.

[4] C. A. Cornell and H. Krawinkler, "Progress and challenges in seismic performance assessment," *PEER Center News*, vol. 3, no. 2, pp. 1–3, 2000.

[5] C. A. Cornell, "Calculating building seismic performance reliability: a basis for multi-level design norms," in *Proceedings of the 11th World Conference on Earthquake Engineering*, Acapulco, Mexico, 1996.

[6] P. Bazzurro, *Probabilistic seismic demand analysis [Ph.D. thesis]*, Department of Civil and Environmental Engineering, Stanford University, Stanford, Calif, USA, 1998.

[7] N. Shome, "Probabilistic seismic demand analysis of nonlinear structures," Tech. Rep. RMS-35, Department of Civil and

Environmental Engineering, Stanford University, Calif, USA, 1999.

[8] P. Bazzurro and C. A. Cornell, "Vector-valued probabilistic seismic hazard analysis (VPSHA)," in *Proceedings of the 7th US national conference on earthquake engineering*, Boston, Mass, USA, 2002.

[9] F. Jalayer and C. A. Cornell, "A technical framework for probability-based demand and capacity factor (DCFD) seismic formats," Tech. Rep. PEER Report 2003/08, Pacific Earthquake Engineering Research Center, University of California, Berkeley, Calif, USA, 2003.

[10] D. Vamvatsikos and C. A. Cornell, "Applied incremental dynamic analysis," *Earthquake Spectra*, vol. 20, no. 2, pp. 523–553, 2004.

[11] K. R. Mackie and B. Stojadinović, "Performance-based seismic bridge design for damage and loss limit states," *Earthquake Engineering & Structural Dynamics*, vol. 36, no. 13, pp. 1953–1971, 2007.

[12] E. M. Rathje and G. Saygili, "Probabilistic seismic hazard analysis for the sliding displacement of slopes: Scalar and vector approaches," *Journal of Geotechnical and Geoenvironmental Engineering*, vol. 134, no. 6, pp. 804–814, 2008.

[13] L. Eads, E. Miranda, H. Krawinkler, and D. G. Lignos, "An efficient method for estimating the collapse risk of structures in seismic regions," *Earthquake Engineering & Structural Dynamics*, vol. 42, no. 1, pp. 25–41, 2013.

[14] J. W. Baker and C. A. Cornell, "Choice of a vector of ground motion intensity measures for seismic demand hazard analysis," in *Proceedings of the Paper presented at 13th World Conference on Earthquake Engineering*, 2004.

[15] P. Tothong and C. A. Cornell, "Application of nonlinear static analyses to probabilistic seismic demand analysis," in *Proceedings of the 8th US National Conference on Earthquake Engineering*, San Francisco, Calif, USA, 2006.

[16] P. Tothong and N. Luco, "Probabilistic seismic demand analysis using advanced ground motion intensity measures," *Earthquake Engineering & Structural Dynamics*, vol. 36, no. 13, pp. 1837–1860, 2007.

[17] P. Tothong, *Probabilistic seismic demand analysis using advanced ground motion intensity measures, attenuation relationships, and near-fault effects [Ph.D. thesis]*, Stanford University, 2007.

[18] D.-G. Lu, X.-H. Yu, F. Pan, and G.-Y. Wang, "Probabilistic seismic demand analysis considering random system properties by an improved cloud method," in *Proceedings of the 14th World Conference on Earthquake Engineering*, Beijing, China, 2008.

[19] E. Miranda and S. Taghavi, "Approximate floor acceleration demands in multistory buildings. I: Formulation," *Journal of Structural Engineering*, vol. 131, no. 2, pp. 203–211, 2005.

[20] J. Wieser, *Assessment of floor accelerations in yielding buildings [M.Sc.Thesis]*, University of Nevada, Reno, 2011.

[21] S. Soroushian, A. E. Zaghi, M. Maragakis, A. Echevarria, Y. Tian, and A. Filiatrault, "Seismic fragility study of fire sprinkler piping systems," in *Proceedings of the Structures Congress 2013, ASCE*, pp. 1533–1544, Pittsburgh, Penn, USA, May 2013.

[22] Y. Tian, A. Filiatrault, and G. Mosqueda, "Experimental seismic study of pressurized fire sprinkler piping subsystems," Tech. Rep. Report MCEER-13-000, University at Buffalo, the State University of New York, Buffalo, NY, USA, 2013.

[23] J. B. Mander, R. P. Dhakal, N. Mashiko, and K. M. Solberg, "Incremental dynamic analysis applied to seismic financial risk assessment of bridges," *Engineering Structures*, vol. 29, no. 10, pp. 2662–2672, 2007.

[24] B. A. Bradley, R. P. Dhakal, M. Cubrinovski, J. B. Mander, and G. A. MacRae, "Improved seismic hazard model with application to probabilistic seismic demand analysis," *Earthquake Engineering & Structural Dynamics*, vol. 36, no. 14, pp. 2211–2225, 2007.

[25] B. A. Bradley, M. Cubrinovski, R. P. Dhakal, and G. A. MacRae, "Probabilistic seismic performance and loss assessment of a bridge-foundation-soil system," *Soil Dynamics and Earthquake Engineering*, vol. 30, no. 5, pp. 395–411, 2010.

[26] Z.-H. Zeng, J. Fan, and Q.-Q. Yu, "Performance-based probabilistic seismic demand analysis of bridge structures," *Engineering Mechanics*, vol. 29, no. 3, pp. 156–162, 2012 (Chinese).

[27] J. C. Wilson and B. S. Tan, "Bridge abutments: Formulation of simple model for earthquake response analysis," *Journal of Engineering Mechanics*, vol. 116, no. 8, pp. 1828–1837, 1990.

[28] K. Mackie and B. Stojadinović, "Probabilistic seismic demand model for California highway bridges," *Journal of Bridge Engineering*, vol. 6, no. 6, pp. 468–481, 2001.

[29] P. Gardoni, A. Der Kiureghian, and K. M. Mosalam, "Probabilistic capacity models and fragility estimates for reinforced concrete columns based on experimental observations," *Journal of Engineering Mechanics*, vol. 128, no. 10, pp. 1024–1038, 2002.

[30] B. G. Nielson and R. DesRoches, "Influence of modeling assumptions on the seismic response of multi-span simply supported steel girder bridges in moderate seismic zones," *Engineering Structures*, vol. 28, no. 8, pp. 1083–1092, 2006.

[31] B. G. Nielson and R. DesRoches, "Analytical seismic fragility curves for typical bridges in the central and southeastern United States," *Earthquake Spectra*, vol. 23, no. 3, pp. 615–633, 2007.

[32] G. P. Cimellaro, A. M. Reinhorn, M. Bruneau, and A. Rutenberg, "Multi-Dimensional Fragility of Structures: Formulation and Evaluation," Tech. Rep. Report MCEER-06-0002, University at Buffalo, State University of New York, Buffalo, NY, USA, 2006.

[33] Q. Wang, Z. Wu, and S. Liu, "Seismic fragility analysis of highway bridges considering multi-dimensional performance limit state," *Earthquake Engineering and Engineering Vibration*, vol. 11, no. 2, pp. 185–193, 2012.

[34] G. P. Cimellaro and A. M. Reinhorn, "Multidimensional performance limit state for hazard fragility functions," *Journal of Engineering Mechanics*, vol. 137, no. 1, pp. 47–60, 2010.

[35] R. W. Clough and J. Penzien, *Dynamics of Structures*, McGraw-Hill, New York, NY, USA, 2nd edition, 1993.

[36] G. P. Cimellaro, H. Roh, and A. De Stefano, "Spectral and fragility evaluations of retrofitted structures through strength reduction and enhanced damping," *Earthquake Engineering and Engineering Vibration*, vol. 8, no. 1, pp. 115–125, 2009.

[37] C. A. Cornell, F. Jalayer, R. O. Hamburger, and D. A. Foutch, "Probabilistic basis for 2000 SAC federal emergency management agency steel moment frame guidelines," *Journal of Structural Engineering*, vol. 128, no. 4, pp. 526–533, 2002.

[38] Y. Zhang, Y. Liu, X. Yang, and Z. Yue, "A global nonprobabilistic reliability sensitivity analysis in the mixed aleatory-epistemic uncertain structures," *Proceedings of the Institution of Mechanical Engineers, Part G: Journal of Aerospace Engineering*, vol. 228, no. 10, pp. 1802–1814, 2014.

[39] C. Jiang, R. G. Bi, G. Y. Lu, and X. Han, "Structural reliability analysis using non-probabilistic convex model," *Computer Methods Applied Mechanics and Engineering*, vol. 254, pp. 83–98, 2013.

[40] Y. J. Luo, Z. Kang, and A. Li, "Structural reliability assessment based on probability and convex set mixed model," *Computers & Structures*, vol. 87, no. 21-22, pp. 1408–1415, 2009.

[41] C. Jiang, X. Han, G. Y. Lu, J. Liu, Z. Zhang, and Y. C. Bai, "Correlation analysis of non-probabilistic convex model and corresponding structural reliability technique," *Computer Methods Applied Mechanics and Engineering*, vol. 200, no. 33–36, pp. 2528–2546, 2011.

[42] B. G. Nielson and R. Desroches, "Seismic performance assessment of simply supported and continuous multispan concrete girder highway bridges," *Journal of Bridge Engineering*, vol. 12, no. 5, pp. 611–620, 2007.

[43] B. G. Nielson, *Analytical Fragility Curves for Highway Bridges in Moderate Seismic Zones [Ph.D. thesis]*, Georgia Institute of Technology, Atlanta, Ga, USA, 2005.

[44] PRC National Code GB50011-2008, *Code for seismic design of buildings*, China Architecture & Building Press, Peaking, China, 2008.

[45] S. Mazzoni, F. McKenna, M. H. Scott, and G. L. Fenves, *OpenSees version 1.7.3 command language manual*, Pacific Earthquake Engineering Research Center, University of California, Berkeley, Calif, USA, 2006.

[46] J. W. Baker and C. A. Cornell, "A vector-valued ground motion intensity measure consisting of spectral acceleration and epsilon," *Earthquake Engineering & Structural Dynamics*, vol. 34, no. 10, pp. 1193–1217, 2005.

[47] J. W. Baker, "Conditional mean spectrum: tool for ground-motion selection," *Journal of Structural Engineering*, vol. 137, no. 3, pp. 322–331, 2011.

[48] N. A. Abrahamson and W. J. Silva, "Empirical response spectral attenuation relations for shallow crustal earthquakes," *Seismological Research Letters*, vol. 68, no. 1, pp. 94–109, 1997.

[49] J. W. Baker and C. A. Cornell, "Which spectral acceleration are you using?" *Earthquake Spectra*, vol. 22, no. 2, pp. 293–312, 2006.

[50] China earthquake administration (CEA), "Zoning map of earthquake ground motion parameters in China (GB18306-2001)," 2001.

[51] China Earthquake Administration (CEA), "Evaluation of seismic safety of engineering sites (GB17741-2005)," 2005.

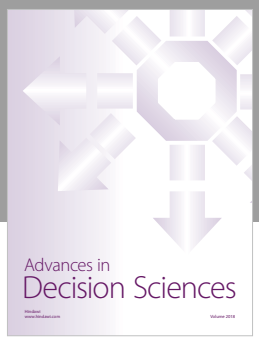

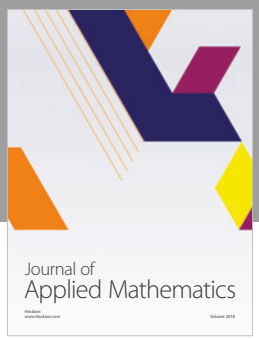

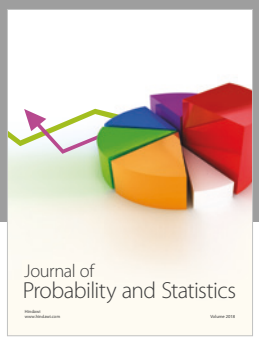

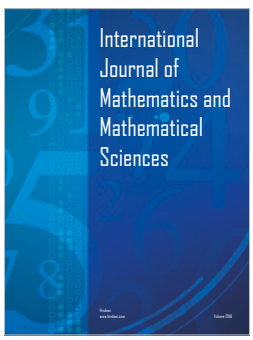

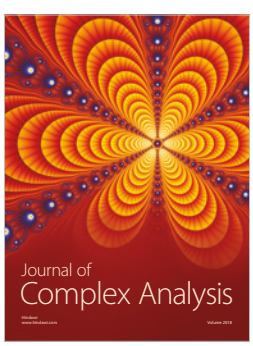

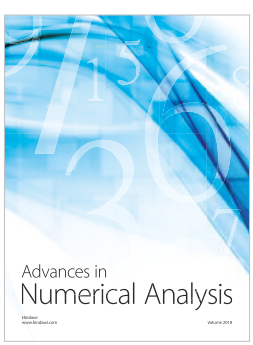

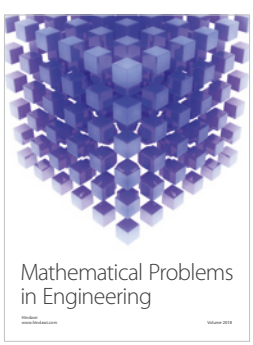

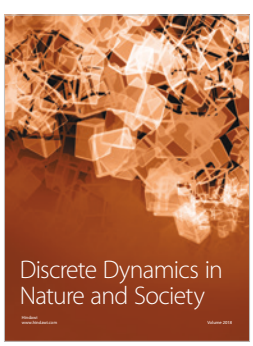

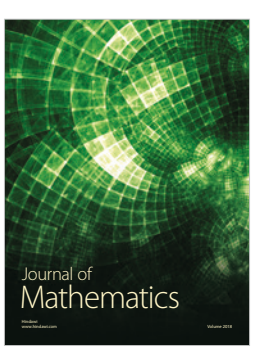

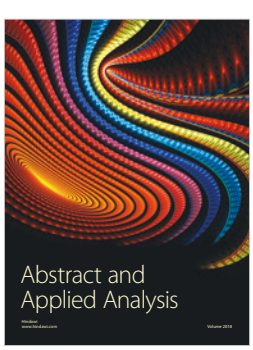

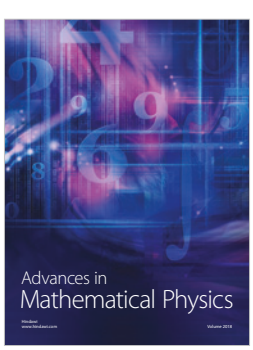

Hindawi

Submit your manuscripts at
www.hindawi.com